

See discussions, stats, and author profiles for this publication at: <https://www.researchgate.net/publication/278043952>

Installing Logic Gates to Multiresponsive Supramolecular Hydrogel Co-assembled from Phenylalanine Amphiphile and Bis(pyridinyl) Derivative

ARTICLE *in* LANGMUIR · JUNE 2015

Impact Factor: 4.46 · DOI: 10.1021/acs.langmuir.5b01585 · Source: PubMed

READS

40

3 AUTHORS:



Guofeng Liu

Shanghai Jiao Tong University

12 PUBLICATIONS 31 CITATIONS

[SEE PROFILE](#)



Ji Wei

Shanghai Jiao Tong University

7 PUBLICATIONS 7 CITATIONS

[SEE PROFILE](#)



Chuan Liang Feng

Shanghai Jiao Tong University

75 PUBLICATIONS 1,100 CITATIONS

[SEE PROFILE](#)

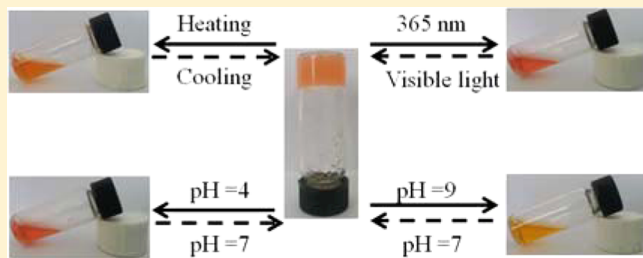
Installing Logic Gates to Multiresponsive Supramolecular Hydrogel Co-assembled from Phenylalanine Amphiphile and Bis(pyridinyl) Derivative

Guo-Feng Liu, Wei Ji, and Chuan-Liang Feng*

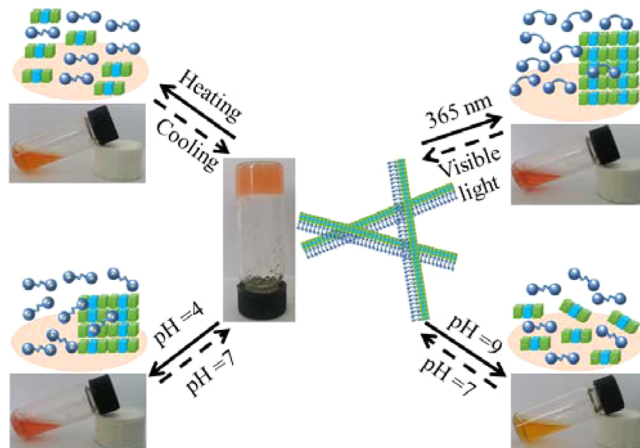
State Key Laboratory of Metal Matrix Composites, School of Materials Science and Engineering, Shanghai Jiaotong University, 800 Dongchuan Road, Shanghai 200240, People's Republic of China

S Supporting Information

ABSTRACT: Recently, logic gates based on multiresponsive hydrogel systems are attractive because of their potential biological applications. A quite simple supramolecular hydrogel co-assembled from phenylalanine-based amphiphile (LPF2) and bis(pyridinyl) derivative (AP) is constructed. The co-assembled hydrogel exhibited a macroscopic gel–sol transition in response to four distinct input stimuli: temperature, acid, base, and light. A set of techniques including microscopic, spectroscopic, and rheological measurements demonstrate this performance and confirm that the hydrogel is formed through intermolecular hydrogen bonds between amide/pyridine moieties and carbonyl groups. On the basis of its multiple-stimulus responsiveness, installing gel-based supramolecular logic gates (OR and XOR) is achieved. It may promote the possibility to develop smart soft materials, such as gels, that can be used as tools releasing a drug quantitatively by rational design and fine control of the external stimuli.



Scheme 1. Schematic Representation of the Multiresponsive Properties of Supramolecular Hydrogel LPF2-AP



INTRODUCTION

Logic gates^{1–6} can be constructed in a multiresponsive supramolecular gel^{7–17} system, where two chemical input signals can be used to control the sol–gel transition.^{18–22} Particularly, hydrogel materials with the ability to function under aqueous conditions are attractive because of their potential biological applications.^{23–31} However, only a few multiresponsive hydrogel systems have been successfully developed.^{32,33} To date, constructing an efficient hydrogel system exhibiting multiresponsive properties still poses a challenge.³²

Alternatively, this challenge may be overcome by supramolecular gels co-assembled from several different molecular building blocks,^{33–41} which may introduce various stimuli-responsive groups into the gels, ensuring their remarkable stimuli-responsive abilities; e.g., the constructed logic gates are prepared by choosing responsive groups, in which two chemical input signals can control the sol–gel transition.²²

Previously, we have found that L-phenylalanine-based amphiphile (LPF2) and azobenzene derivative can co-assemble into nanofibers and form hydrogel with multistimuli responses for photoguiding cell detachment and release.³³ Inspired from the above co-assembled hydrogel system, a multiresponsive hydrogel co-assembled from LPF2 and bis(pyridinyl) derivative (AP) is constructed, which show sharp phase transitions in response to a series of disparate stimuli (temperature changes, photoirradiation, and pH changes, as seen in Scheme 1). First, besides the thermal responsiveness of the gel, the incorporation of the azobenzene (Azo) group makes it possible to be light-

responsive. In addition, phenylalanine groups from LPF2 and the pyridinyl group in AP provide the dual pH response by both adding acid and base. With the different reversible inputs available and with different ways to reverse these signals, gel-based supramolecular logic gates (OR and XOR) are constructed.

Received: April 30, 2015

Revised: June 3, 2015

Published: June 10, 2015



EXPERIMENTAL SECTION

Materials. All chemicals were purchased from Aldrich and used without further purification. Phenylalanine derivative gelator (LPF2) and azobenzene derivative (AP) were synthesized with a high yield through a conventional liquid-phase reaction according to a previous paper³² and Scheme S1 of the Supporting Information. The synthesis method is described in the Supporting Information. Nuclear magnetic resonance (NMR) experiments were performed using a Bruker Advance III 400 instrument operated at 400 MHz. Fast atom bombardment mass spectrometry (FABMS) spectra were obtained by a JEOL JMS 700 mass spectrometer. The concentration of hydrogel was 2.0 mg mL⁻¹.

Gelation. The LPF2–AP hydrogel with 0.2 wt % LPF2–AP is used as an example to describe the preparation procedure. LPF2–AP (2.0 mg mL⁻¹) (equimolar 1:1 mixture of LPF2 and AP) was suspended in a septum-capped 3 mL glass vial and heated (about 100 °C) until the solid was dissolved, after which the solution was allowed to cool to room temperature. Hydrogel was considered to have formed with no gravitational flow upon inversion of the vial.

Scanning Electronic Microscopy (SEM). SEM measurements were carried out using a FEI QUANTA 250 microscope. Samples were prepared by depositing dilute solutions of gel on silicon slice, drying them under vacuum, and coating with gold on a sputtering coater.

Transmission Electron Microscopy (TEM). TEM from Tecnai G2 Spirit Biotwin (FEI, Hillsboro, OR) was used to characterize the nanofibrous xerogels. The LPF2–AP samples for TEM observation were prepared by placing drops of the diluted LPF2–AP aqueous suspension onto copper grids, which were then dried under ambient conditions prior to being introduced into the TEM chamber (JEM-2010).

Circular Dichroism (CD) Spectroscopy. CD spectra were collected on a JASCO J-815 CD spectrometer with bandwidth of 1.0 nm. CD spectra of hydrogels were recorded in the ultraviolet (UV) region (190–400 nm) using a 0.1 mm quartz cuvette with the total gelator concentration at 0.2 wt %.

Rheological Measurements. The rheological properties of hydrogels were measured using a rheometer (Gemini HRnano). The measurements were performed using a dynamic frequency sweep test with 0.05% strain over a range of frequencies (0.01–10 Hz) at 25 °C.

Fourier Transform Infrared (FTIR) Spectroscopy. FTIR spectra of xerogels were taken using a Bruker EQUINOX55 instrument. The KBr disk technique was used for the solid-state measurement. The samples were scanned between the wavenumber of 4000 and 400 cm⁻¹ at an interval of 1.9285 cm⁻¹.

X-ray Powder Diffraction (XRD). The XRD patterns were obtained from xerogels. The LPF2 and LPF2–AP hydrogels were filtered and dried upon vacuum to obtain xerogel. The XRD pattern was recorded on a D8 Advance instrument from Bruker Company (step size, 0.02°; step time, 0.8 s).

RESULTS AND DISCUSSION

Co-assembly of LPF2 with AP. The LPF2 have two phenylalanine head groups connected by a phenyl ring via amide bonds (Figure 1a). The hydrogen bonding interactions between the amide groups and the carboxylic acid of the phenylalanine head groups play an important role in the self-assembly process,³³ rendering LPF2 to self-assemble into nanofibers and form transparent hydrogels (Figure 1c) with the critical gelation concentration (CGC) of 0.2% (w/v). SEM images of two-component supramolecular gel (LPF2–AP) clearly displays a uniform fibrillar network in the hydrogels (Figure 1b). The network was composed of well-organized fibrils having widths of 100 nm and maximum lengths of several micrometers.

Co-assembly Mechanism. ¹H NMR was used to explore the co-assembly mechanism of LPF2–AP gel (Figure 2a). Because of the strong electron absorbing effect of the carboxyl

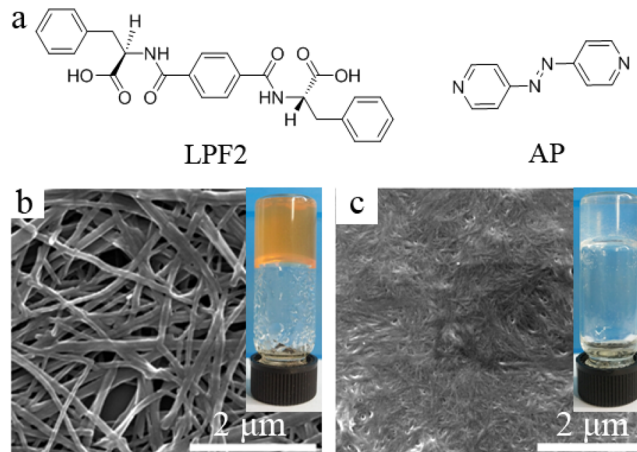


Figure 1. (a) Chemical structures of the gelator LPF2 and azobenzene derivative AP. SEM images of (b) LPF2–AP gel and (c) LPF2 gel. (Inset) Photographs of (b) LPF2–AP hydrogel and (c) LPF2 hydrogel.

groups in the LPF2 structure, the signals of the heteroaromatic protons in AP were steadily shifted downfield (e.g., proton a of the pyridine ring is shifted from 8.60 to 8.74 ppm, and proton b of the pyridine ring is shifted from 7.45 to 7.80 ppm; Figure 2a). It suggested that the hydrogen bonding formed between the pyridinyl moiety and carboxyl group in the co-assembled hydrogel system. The contribution of new hydrogen bonds to the gelation was also confirmed by FTIR spectroscopy (Figure 2b and Figure S2 and Table S1 of the Supporting Information) and CD spectra (see Figure S3 of the Supporting Information). In Figure 2b, a new strong band at 3432 cm⁻¹ was observed in LPF2–AP gel, whereas the peak at 3306 cm⁻¹ assigned to the characteristic associated peak of carboxyl groups in LPF2 gel has disappeared in LPF2–AP gel, which is ascribed to the hydrogen bond formation between pyridinyl moieties and carboxyl groups. In comparison to the CD spectra of LPF2 gels having a negative Cotton effect at 314 nm, the CD spectra of co-assembled gels displayed a positive Cotton effect at 318 nm in the α -helix secondary structure (see Figure S3 of the Supporting Information).³³ Moreover, gels and AP powders were also investigated by XRD measurement (Figure 2c). From the XRD spectra, the characteristic peaks of LPF2–AP (11.3°, 12.2°, 16.5°, and 19.7°) did not show any overlaid peaks of LPF2 (6.6°, 13.8°, 14.7°, 18.4°, and 20.6°) or AP (15°, 17.2°, 23.6°, 25.9°, and 27.6°), which demonstrated that new aggregates were formed and co-assembly occurred. Both results of CD and XRD spectra suggested that the presence of AP had influence on the assembly process in the co-assembled gels. On the basis of these results above and our previous works,³³ there are not only hydrogen bond interactions between amide and carboxyl moieties but also hydrogen bond interactions between pyridinyl and carboxyl moieties in the LPF2–AP system, assembling collaboratively into nanofibers and gelating in water.

Mechanical Enhancement. Figure 3 shows oscillatory rheology data that reports on the mechanical rigidity of LPF2 (2.0 mg mL⁻¹) and LPF2–AP (L-PF2 + AP = 2.0 mg mL⁻¹) hydrogels. In a dynamic strain sweep to gels, the values of the storage modulus (G') and the loss modulus (G'') exhibited a weak dependence from 0.01 to 0.1% of strain (G' dominating G''), indicating that both of the samples are gels. The variation of the storage modulus (G') and loss modulus (G'') was monitored as a function of applied angular frequency under a

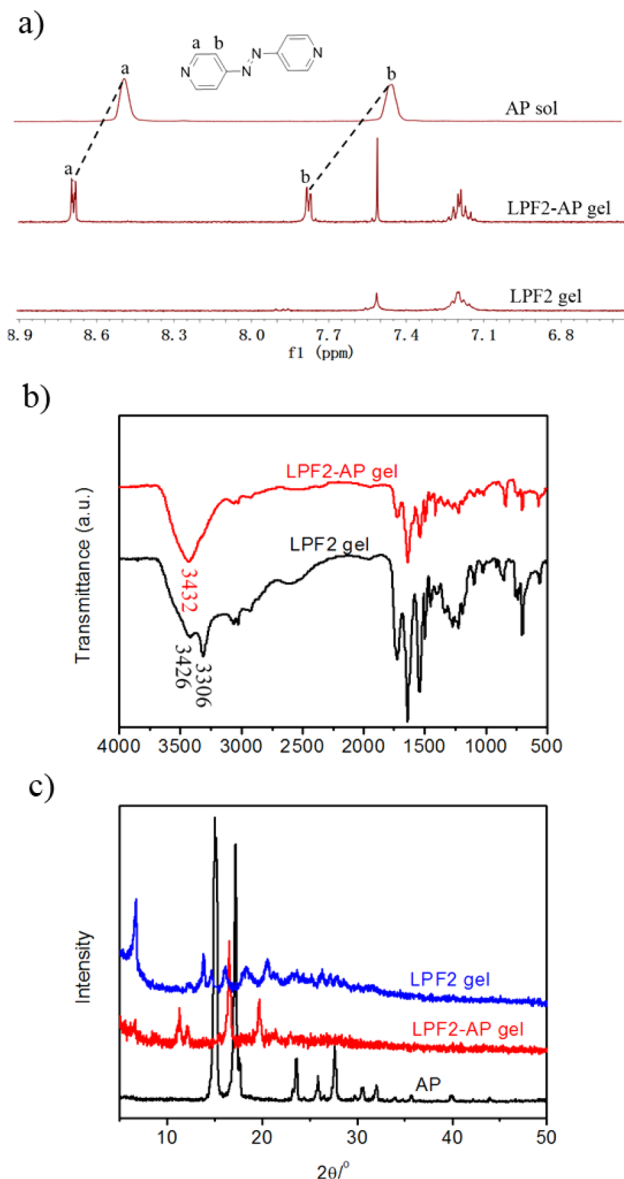


Figure 2. (a) ${}^1\text{H}$ NMR spectra of (top) AP, (middle) LPF2-AP gel, and (bottom) LPF2 gel in D_2O . (b) FTIR curves of LPF2-AP xerogel and LPF2 xerogel. (c) X-ray powder diffraction of the LPF2 xerogel, LPF2-AP xerogel, and AP powder.

constant strain of 0.05%. Figure 3b shows the linear viscoelastic frequency sweep responses of these hydrogels. The storage modulus (G') of the hydrogels was larger than the loss modulus (G''), indicating that the hydrogels are typically elastic rather than viscous soft matter. In addition, the variation of dynamic moduli (G' and G'') versus time after gelation at 20 °C is shown in Figure 3c. The modulus values are kept constant within a long period of time, indicating the stability of the hydrogel networks. In comparison to LPF2 hydrogels, LPF2-AP hydrogels showed much better mechanical rigidity. In this case, the storage modulus (G') of LPF2-AP hydrogels (~600 Pa) was 3-fold greater than that of LPF2 hydrogels (~200 Pa). Because the critical gelation concentration of LPF2 was 2.0 mg mL $^{-1}$, the concentration of LPF2 in LPF2-AP was only 1.4 mg mL $^{-1}$, which cannot even make LPF2 form hydrogels alone. It means that the increased mechanical properties for LPF2-AP should be ascribed to the hydrogen bonding between LPF2 and

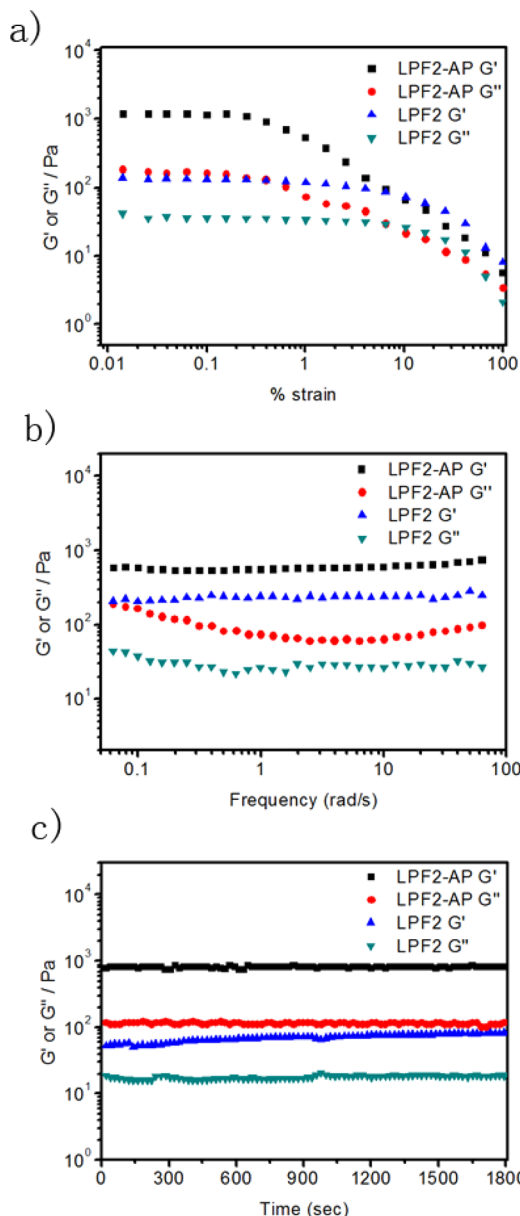


Figure 3. Rheological measurement of the (a) strain sweep at a frequency of 1 rad $^{-1}$, (b) frequency sweep at a strain of 0.05%, and (c) time sweep at a frequency of 1 rad $^{-1}$ and a strain of 0.05% of hydrogels LPF2 and LPF2-AP at 25 °C.

AP. For the two-component hydrogels, AP may work as “glue”, which can connect LPF2 molecules and promote the gelation process.

Response to Temperature and pH. The thermoresponsive property of LPF2-AP hydrogel was directly confirmed by the dissolution with an increasing temperature and gelation again upon cooling (Scheme 1). In addition, LPF2-AP is soluble in dimethyl sulfoxide (DMSO), and when water was added to a solution of LPF2-AP in DMSO, orange gels were formed quickly at room temperature. The gels transformed into a solution upon heating and formed again after cooling.

The hydrogen bonding interactions between pyridinyl and carboxyl groups cannot only produce the co-assembled nanofibers but also provide interesting dual pH responsive ability in both acid and base (Figure 4a).^{43,44} When the pH value was 7, LPF2-AP could form a stable gel. When the pH

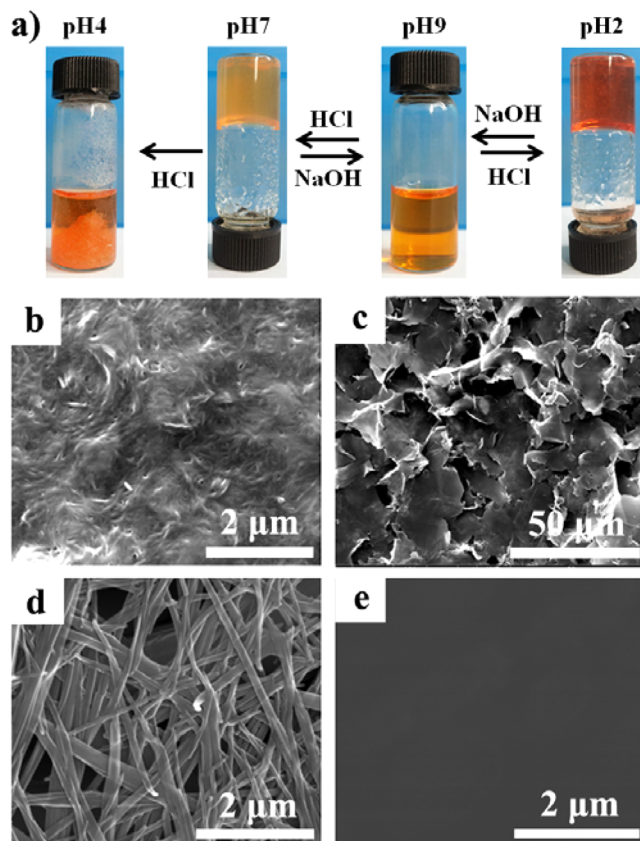


Figure 4. (a) Gel–sol transition of the multicomponent hydrogels LPF2–AP triggered by both acid and base. SEM images of LPF2–AP gel at (b) pH 2, (c) pH 4, (d) pH 7, and (e) pH 9.

value of the systems was changed to 4, the hydrogels would become orange precipitates. When the pH was changed to 9, yellow green solution was obtained. In the case of a high pH value, the basic solution could turn back to the gel and the process was reversible (Figure 4a). Once the pH value of the systems was tailored to 2, rust red hydrogels formed. However, LPF2 hydrogels can also transform into solution at a higher pH value after adding base, and the gel–sol transformation cannot be triggered below pH 7 (see Figure S4 of the Supporting Information).

The self-assembled structures formed were found to depend upon the pH of the system. At a pH of 2, below both pK_a values of pyridinyl ($pK_a = 5.25$) and carboxyl ($pK_a = 2.20$) groups,^{45,46} well-organized and slender fibrils were observed in the SEM image, which were due to the self-assembly of LPF2 (Figure 4b). At pH 4, precipitate formed and lamellar sheets were observed in the SEM image (Figure 4c). At a pH of 7, SEM images exhibited well-organized and thick fibrils co-assembled from LPF2 and AP in Figure 4d. At pH 9, LPF2–AP exists in its liquid state, with the SEM image showing neither fibers nor lamellar sheets (Figure 4e).

The color changes of azobenzene chromophores upon pH changes were further studied by UV–vis spectroscopy (see Figure S5 of the Supporting Information). When pH changes, the protonation of the pyridinyl groups in solution occurred, as evidenced by the spectral changes. As shown in Figure S5 of the Supporting Information, along with the increase of the pH value, a gradual decrease of the intensity of absorption at 275 nm and the concomitant new peak at 280 nm band were observed, indicating the progress of the deprotonation. These

spectral changes were well-related to the color change of the macroscopic state of the sample observed. These results from both UV–vis spectroscopy and photo images indicated that the protonation of pyridinyl and ionization of carboxyl moieties gave rise to the gel–sol transition upon pH changes.

Response to Photoirradiation. As the photoisomerization property of the Azo units, the gel–sol phase transitions could be further triggered by light. Upon UV (365 nm) irradiation, the stable orange gels were found to collapse gradually. In addition, the UV irradiation also caused the morphology change of the gel system (Figure 5a). Microscopic images of the

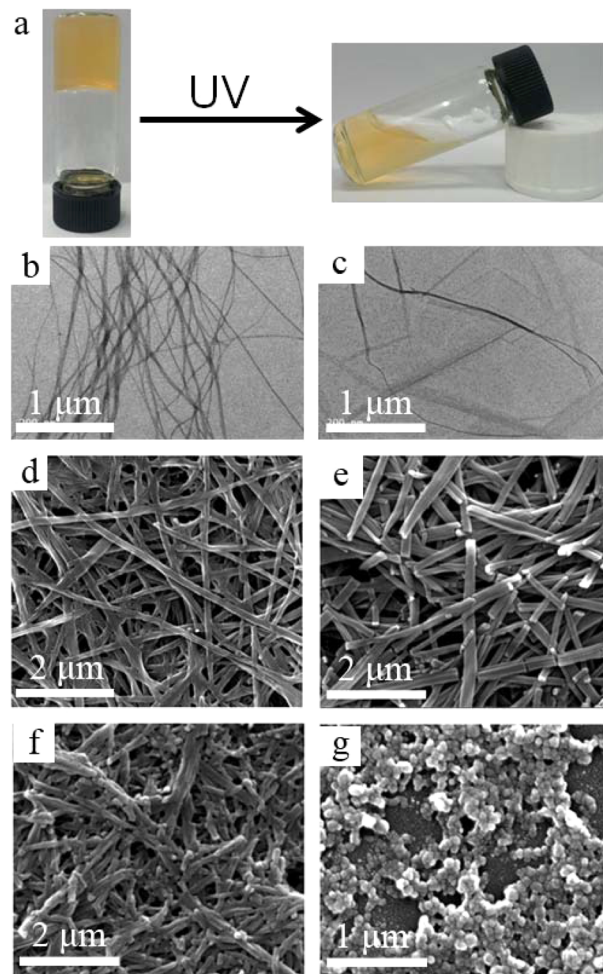


Figure 5. (a) Photographs of LPF2–AP gel before and after UV irradiation. TEM images of LPF2–AP gel (b) before and (c) after UV irradiation. SEM images of LPF2–AP gel under UV irradiation for (d) 0 min, (e) 30 min, (f) 60 min, and (g) 10 h.

LPF2–AP xerogels (panels b and d of Figure 5) confirmed that the hydrogels were composed of the well-organized fibrils having widths of 100 nm and maximum lengths up to 100 μm in both SEM and TEM images (panels b and d of Figure 5). After UV irradiation for 30 min, the broken fibers and corresponding degradation of the fibrous network were observed (panels c and e of Figure 5). More interestingly, as shown in panels d–g of Figure 5, along with the elongation of irradiation time, a gradual decrease of the length of the fibers and the increase of broken fibers and concomitant nanoparticles with diameters at 100 nm were observed after exposure under UV light for 10 h, indicating the whole

progress of the photoisomerization of Azo and gel disassembly. Thus, UV irradiation disrupted the molecular packing of gelator LPF2-AP, followed by dissociation of the fibers and their three-dimensional networks of the gel.

Therefore, the co-assembled hydrogels exhibited sharp phase transitions in response to a series of disparate stimuli as follows. First, the gel transformed to solution upon heating and formed gel again after cooling. Second, the protonation of pyridinyl and ionization of carboxyl moieties gave rise to the gel-sol transition upon the addition of either acid or base. Finally, UV irradiation can induce the photoisomerization of AP, followed by disrupting the molecular packing of LPF2-AP and dissociating the fibers and three-dimensional networks of the gel.

Construction of Logic Gates. Because of the reversible multiresponsive properties of LPF2-AP hydrogels, logic gates are constructed, which connect two different inputs to the gel-sol or sol-gel transition as the output. All gates presented below are based on the same output assignment to avoid confusion: the gel state corresponds to "0", and the sol state corresponds to "1". The assignment can be reversed without problems and would, for example, transfer the NOR gate into an OR gate and vice versa.

For the XOR gate, it is necessary to find inputs that cancel each other out. Consequently, the addition of NaOH and HCl come into play here (Figure 6). A single input destroys the gel,

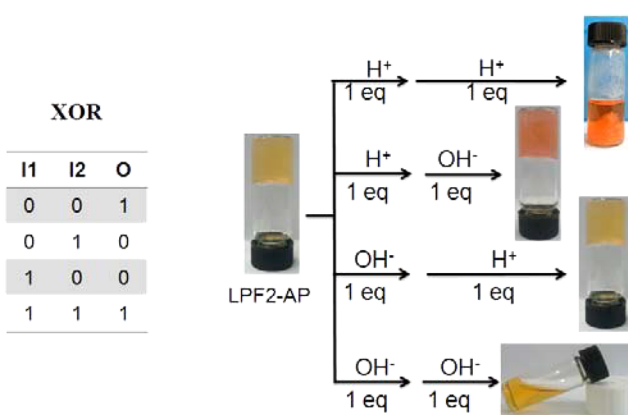


Figure 6. XOR logic gate constructed from the LPF2-AP gel. The two input signals are OH^- and H^+ , respectively. All gates are based on the same output definition: gel = 0, and sol = 1.

be it the OH^- ion or the H^+ ion. If, however, both inputs are present, the acid-base neutralization keeps pH at 7 and the gel reforms. As discussed above, the complete destruction of the gel requires tuning pH to 4 or 9. Consequently, the same amount of base and acid is necessary for reliable operation of the gate. The input signals are OH^- (NaOH , 5×10^{-4} mol/L) and H^+ (HCl , 5×10^{-4} mol/L). If one adds 2 equiv of acid to tailor pH at 4 ($I = 0$ and 0), the pyridinyl group is protonated and the sol and precipitates are obtained ($O = 1$). When 1 equiv of base and 1 equiv of acid are added ($I = 0$ and 1), the pH is kept at 7, the gel is restored, and the sequence of the addition of acid and base ($I = 1$ and 0) does not change the gel state. If the gel is treated with 2 equiv of base ($I = 1$ and 1), the sol is obtained ($O = 1$) at pH 9. The XOR gate could, thus, be constructed by fine tuning the concentration of the stimuli.

We constructed an OR logic gate (Figure 7) comprising a suitable concentration of LPF2 and AP at neutral pH, for which

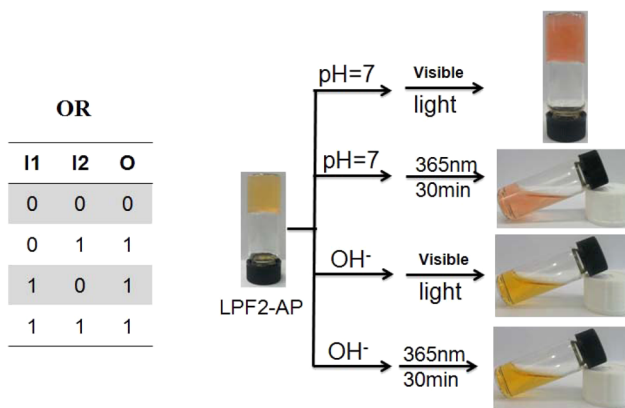


Figure 7. OR logic gate constructed from the LPF2-AP gel. The two input signals are OH^- and UV light, respectively. For consistency, gel = 0 and sol = 1.

UV light and base served as the two inputs. The starting state is also a gel ($O = 0$). If one adds enough base but without UV light irradiation ($I = 1$ and 0), the carboxyl group is ionized and then the sol is obtained ($O = 1$). When, under UV light, base is added ($I = 1$ and 1), the sol is obtained again. If the gel is treated without UV light irradiation at pH 7 ($I = 0$ and 0), the gel remains a gel ($O = 1$). While the gel is treated with UV light irradiation at pH 7 ($I = 0$ and 0), the sol is obtained again. To construct the OR gate, the addition of OH^- and UV light to either one input is required. Adding OH^- or UV light induces the gel-sol phase transition, as does the treating of both.

CONCLUSION

In summary, a multiresponsive hydrogel system, responded to the temperature, photoirradiation, and acid and base, was constructed through the co-assembly of LPF2 and AP for installing logic gates. Interestingly, dependent upon the choice of components of the system and fine tune of the stimuli concentrations of input signals, different logic gates (XOR and OR) can be constructed from the same system. Thus, the proof-of-concept of such logic gates may promote the possibility to develop smart materials, such as gels that can be used as tools, releasing a drug quantitatively by rational design and fine control of the external stimuli.

ASSOCIATED CONTENT

Supporting Information

Synthetic route, optical pictures, ^1H NMR, FTIR, and CD spectra (PDF). The Supporting Information is available free of charge on the ACS Publications website at DOI: 10.1021/acs.langmuir.5b01585.

AUTHOR INFORMATION

Corresponding Author

*Fax: +86-2154747651. E-mail: clfeng@sjtu.edu.cn.

Notes

The authors declare no competing financial interest.

ACKNOWLEDGMENTS

This work was financially supported by the National Science Foundation of China (51173105 and 51273111) and the National Basic Research Program of China (973 Program, 2012CB933803).

■ REFERENCES

- (1) de Silva, P. A.; Gunaratne, N. H. Q.; McCoy, C. P. A molecular photoionic AND gate based on fluorescent signalling. *Nature* **1993**, *364* (6432), 42–44.
- (2) Collier, C. P.; Wong, E. W.; Belohradský, M.; Raymo, F. M.; Stoddart, J. F.; Kuekes, P. J.; Williams, R. S.; Heath, J. R. Electronically configurable molecular-based logic gates. *Science* **1999**, *285* (5426), 391–394.
- (3) Credi, A.; Balzani, V.; Langford, S. J.; Stoddart, J. F. Logic operations at the molecular level. An XOR gate based on a molecular machine. *J. Am. Chem. Soc.* **1997**, *119* (11), 2679–2681.
- (4) Okamoto, A.; Tanaka, K.; Saito, I. DNA logic gates. *J. Am. Chem. Soc.* **2004**, *126* (30), 9458–9463.
- (5) Qu, D. H.; Wang, Q. C.; Tian, H. A half adder based on a photochemically driven [2]rotaxane. *Angew. Chem., Int. Ed.* **2005**, *44* (33), 5296–5299.
- (6) Meng, F.; Hervault, Y. M.; Shao, Q.; Hu, B.; Norel, L.; Rigaut, S.; Chen, X. Orthogonally modulated molecular transport junctions for resettable electronic logic gates. *Nat. Commun.* **2014**, *5*, 1–9.
- (7) Li, J.; Cvrtila, I.; Colomb-Delsuc, M.; Otten, E.; Otto, S. An “ingredients” approach to functional self-synthesizing materials: A metal-ion-selective, multi-responsive, self-assembled hydrogel. *Chem.—Eur. J.* **2014**, *20* (48), 15709–15714.
- (8) Liu, J.; He, P.; Yan, J.; Fang, X.; Peng, J.; Liu, K.; Fang, Y. An organometallic super-gelator with multiple-stimulus responsive properties. *Adv. Mater.* **2008**, *20* (13), 2508–2511.
- (9) Wang, C.; Chen, Q.; Sun, F.; Zhang, D.; Zhang, G.; Huang, Y.; Zhao, R.; Zhu, D. Multistimuli responsive organogels based on a new gelator featuring tetrathiafulvalene and azobenzene groups: Reversible tuning of the gel–sol transition by redox reactions and light irradiation. *J. Am. Chem. Soc.* **2010**, *132* (9), 3092–3096.
- (10) Duan, P.; Li, Y.; Li, L.; Deng, J.; Liu, M. Multiresponsive chiroptical switch of an azobenzene-containing lipid: Solvent, temperature, and photoregulated supramolecular chirality. *J. Phys. Chem. B* **2011**, *115* (13), 3322–3329.
- (11) Yan, X.; Xu, D.; Chi, X.; Chen, J.; Dong, S.; Ding, X.; Yu, Y.; Huang, F. A multiresponsive, shape-persistent, and elastic supramolecular polymer network gel constructed by orthogonal self-assembly. *Adv. Mater.* **2012**, *24* (3), 362–369.
- (12) Dong, S.; Zheng, B.; Xu, D.; Yan, X.; Zhang, M.; Huang, F. A crown ether appended super gelator with multiple stimulus responsiveness. *Adv. Mater.* **2012**, *24* (24), 3191–3195.
- (13) Liu, Z.-X.; Feng, Y.; Yan, Z.-C.; He, Y.-M.; Liu, C.-Y.; Fan, Q.-H. Multistimuli responsive dendritic organogels based on azobenzene-containing poly(aryl ether) dendron. *Chem. Mater.* **2012**, *24* (19), 3751–3757.
- (14) Fatás, P.; Bachl, J.; Oehm, S.; Jiménez, A. I.; Cativiela, C.; Díaz Díaz, D. Multistimuli-responsive supramolecular organogels formed by low-molecular-weight peptides bearing side-chain azobenzene moieties. *Chem.—Eur. J.* **2013**, *19* (27), 8861–8874.
- (15) Jiang, Y.; Zeng, F.; Gong, R.; Guo, Z.; Chen, C.-F.; Wan, X. A multi-stimuli responsive organogel based on a tetrapeptide–dithienylcyclopentene conjugate. *Soft Matter* **2013**, *9* (31), 7538–7544.
- (16) Yang, R.; Peng, S.; Hughes, T. C. Multistimuli responsive organogels based on a reactive azobenzene gelator. *Soft Matter* **2014**, *10* (13), 2188–2196.
- (17) Lakshmi, N. V.; Mandal, D.; Ghosh, S.; Prasad, E. Multi-stimuli-responsive organometallic gels based on ferrocene-linked poly(aryl ether) dendrons: Reversible redox switching and Pb²⁺-ion sensing. *Chem.—Eur. J.* **2014**, *20* (29), 9002–9011.
- (18) Ikeda, M.; Tanida, T.; Yoshii, T.; Kurotani, K.; Onogi, S.; Urayama, K.; Hamachi, I. Installing logic-gate responses to a variety of biological substances in supramolecular hydrogel–enzyme hybrids. *Nat. Chem.* **2014**, *6* (6), 511–518.
- (19) Komatsu, H.; Matsumoto, S.; Tamaru, S.-i.; Kaneko, K.; Ikeda, M.; Hamachi, I. Supramolecular hydrogel exhibiting four basic logic gate functions to fine-tune substance release. *J. Am. Chem. Soc.* **2009**, *131* (15), 5580–5585.
- (20) Ma, X.; Wang, Q.; Qu, D.; Xu, Y.; Ji, F.; Tian, H. A light-driven pseudo[4]rotaxane encoded by induced circular dichroism in a hydrogel. *Adv. Funct. Mater.* **2007**, *17* (5), 829–837.
- (21) Zhu, L.; Ma, X.; Ji, F.; Wang, Q.; Tian, H. Effective enhancement of fluorescence signals in rotaxane-doped reversible hydrogel–gel systems. *Chem.—Eur. J.* **2007**, *13* (33), 9216–9222.
- (22) Qi, Z.; Malo de Molina, P.; Jiang, W.; Wang, Q.; Nowosinski, K.; Schulz, A.; Gradzielski, M.; Schalley, C. A. Systems chemistry: Logic gates based on the stimuli-responsive gel–sol transition of a crown ether-functionalized bis(urea) gelator. *Chem. Sci.* **2012**, *3* (6), 2073–2082.
- (23) Estroff, L. A.; Hamilton, A. D. Water gelation by small organic molecules. *Chem. Rev.* **2004**, *104* (3), 1201–1218.
- (24) Hirst, A. R.; Escuder, B.; Miravet, J. F.; Smith, D. K. High-tech applications of self-assembling supramolecular nanostructured gel-phase materials: From regenerative medicine to electronic devices. *Angew. Chem., Int. Ed.* **2008**, *47* (42), 8002–8018.
- (25) Xu, B. Gels as functional nanomaterials for biology and medicine. *Langmuir* **2009**, *25* (15), 8375–8377.
- (26) Jayawarna, V.; Ali, M.; Jowitt, T. A.; Miller, A. F.; Saiani, A.; Gough, J. E.; Ulijn, R. V. Nanostructured hydrogels for three-dimensional cell culture through self-assembly of fluorenylmethoxy-carbonyl–dipeptides. *Adv. Mater.* **2006**, *18* (5), 611–614.
- (27) Ikeda, M.; Ochi, R.; Hamachi, I. Supramolecular hydrogel-based protein and chemosensor array. *Lab Chip* **2010**, *10* (24), 3325–3334.
- (28) Ikeda, M.; Yoshii, T.; Matsui, T.; Tanida, T.; Komatsu, H.; Hamachi, I. Montmorillonite–supramolecular hydrogel hybrid for fluorocolorimetric sensing of polyamines. *J. Am. Chem. Soc.* **2011**, *133* (6), 1670–1673.
- (29) Yang, Z.; Xu, B. A simple visual assay based on small molecule hydrogels for detecting inhibitors of enzymes. *Chem. Commun.* **2004**, *21*, 2424–2425.
- (30) Yang, Z. M.; Xu, K. M.; Guo, Z. F.; Guo, Z. H.; Xu, B. Intracellular enzymatic formation of nanofibers results in hydrogelation and regulated cell death. *Adv. Mater.* **2007**, *19* (20), 3152–3156.
- (31) Li, X.; Li, J.; Gao, Y.; Kuang, Y.; Shi, J.; Xu, B. Molecular nanofibers of olsalazine form supramolecular hydrogels for reductive release of an anti-inflammatory agent. *J. Am. Chem. Soc.* **2010**, *132* (50), 17707–17709.
- (32) Sun, Z.; Li, Z.; He, Y.; Shen, R.; Deng, L.; Yang, M.; Liang, Y.; Zhang, Y. Ferrocenoyl phenylalanine: A new strategy toward supramolecular hydrogels with multistimuli responsive properties. *J. Am. Chem. Soc.* **2013**, *135* (36), 13379–13386.
- (33) Liu, G. F.; Ji, W.; Wang, W.-L.; Feng, C. L. Multiresponsive hydrogel coassembled from phenylalanine and azobenzene derivatives as 3D scaffolds for photoguiding cell adhesion and release. *ACS Appl. Mater. Interfaces* **2015**, *7* (1), 301–307.
- (34) Buerkle, L. E.; Rowan, S. J. Supramolecular gels formed from multi-component low molecular weight species. *Chem. Soc. Rev.* **2012**, *41* (18), 6089–6102.
- (35) Smith, M. M.; Edwards, W.; Smith, D. K. Self-organisation effects in dynamic nanoscale gels self-assembled from simple mixtures of commercially available molecular-scale components. *Chem. Sci.* **2013**, *4* (2), 671–676.
- (36) Lee, H. Y.; Nam, S. R.; Hong, J.-I. Microtubule formation using two-component gel system. *J. Am. Chem. Soc.* **2007**, *129* (5), 1040–1041.
- (37) Shen, Z.; Wang, T.; Liu, M. H-bond and π–π stacking directed self-assembly of two-component supramolecular nanotubes: Tuning length, diameter and wall thickness. *Chem. Commun.* **2014**, *50* (17), 2096–2099.
- (38) Hirst, A. R.; Miravet, J. F.; Escuder, B.; Noirez, L.; Castelletto, V.; Hamley, I. W.; Smith, D. K. Self-assembly of two-component gels: Stoichiometric control and component selection. *Chem.—Eur. J.* **2009**, *15* (2), 372–379.
- (39) Hirst, A. R.; Smith, D. K.; Feiters, M. C.; Geurts, H. P. M. Two-component dendritic gel: Effect of stereochemistry on the supramolecular chiral assembly. *Chem.—Eur. J.* **2004**, *10* (23), 5901–5910.

- (40) Huang, B.; Hirst, A. R.; Smith, D. K.; Castelletto, V.; Hamley, I. W. A direct comparison of one- and two-component dendritic self-assembled materials: Elucidating molecular recognition pathways. *J. Am. Chem. Soc.* **2005**, *127* (19), 7130–7139.
- (41) Bairi, P.; Roy, B.; Nandi, A. K. A light harvesting bi-component hydrogel with a riboflavin acceptor. *Chem. Commun.* **2012**, *48* (88), 10850–10852.
- (42) Liu, G. F.; Zhang, D.; Feng, C. L. Control of three-dimensional cell adhesion by the chirality of nanofibers in hydrogels. *Angew. Chem., Int. Ed.* **2014**, *53* (30), 7789–7793.
- (43) Hisamatsu, Y.; Banerjee, S.; Avinash, M. B.; Govindaraju, T.; Schmuck, C. A supramolecular gel from a quadruple zwitterion that responds to both acid and base. *Angew. Chem., Int. Ed.* **2013**, *52* (48), 12550–12554.
- (44) Shen, Z.; Wang, T.; Liu, M. Tuning the gelation ability of racemic mixture by melamine: Enhanced mechanical rigidity and tunable nanoscale chirality. *Langmuir* **2014**, *30* (35), 10772–10778.
- (45) Tang, C.; Smith, A. M.; Collins, R. F.; Ulijn, R. V.; Saiani, A. Fmoc-diphenylalanine self-assembly mechanism induces apparent pK_a shifts. *Langmuir* **2009**, *25* (16), 9447–9453.
- (46) Adams, D. J. Dipeptide and tripeptide conjugates as low-molecular-weight hydrogelators. *Macromol. Biosci.* **2011**, *11* (2), 160–173.